The Influence of Some Secondary Effects on Solar Chimney Power Plant Performance

T.W. von Backström, C.F. Kirstein and L.A. Pillay

A solar chimney power plant consists of a large greenhouse type collector surrounding a tall chimney. Hot air escaping through the chimney first passes through a turbine that powers a generator. The paper compares the effects of collector-to-chimney-transition loss, turbine efficiency, skin friction loss, chimney internal bracing wheel loss and non-adiabatic atmospheric conditions on the performance of solar chimney power plants. New findings were that the chimney bracing wheel rims protruding into the chimney could account for as much as 70 % of the bracing wheel drag, or about 5 % of the turbine pressure drop. Of the effects investigated, the bracing wheel rim drag had the largest effect on pressure drop through the system. With the removal of the bracing wheel rims, as recommended, the only remaining effect larger than 1 % of the turbine pressure drop is the drag of the bracing wheel spokes, and the exit dynamic pressure. When compared to an adiabatic atmospheric model, a standard type atmosphere with a lapse rate of 6.5 K per 1000 m reduces the pressure difference across the turbine by about 11 % for the standard 1500 m tall chimney. This shows that there remains very limited scope for improving the performance of solar chimney power plants by reducing secondary losses in the system. The ultimate lower limit of the system pressure drop is about 1.5 times the chimney exit dynamic pressure. These findings are useful in optimisation studies of solar chimney power plants.

1. Introduction

A solar chimney power plant (Schlaich, 1995) consists of a large greenhouse surrounding a tall chimney. Hot air escaping through the chimney first passes through a turbine that powers a generator, (Figure 1). The secondary effects investigated experimentally in this paper are those associated with the collector-to-chimney transition, the turbine, the chimney bracing wheels, and the effect of the ambient atmospheric lapse rate on the performance of the chimney.

2. Background

Collector size, incident angle of solar radiation and flow velocity are the main variables affecting temperature rise in the collector. The chimney height and the difference between the average air density inside and outside the chimney determine the magnitude of the hydrostatic driving potential. When air moves through the chimney, the vertical flow acceleration along the chimney, and the flow resistance of the system, including that associated with the collector, the transition from collector to chimney, the chimney internal configuration, and the kinetic energy loss at the chimney top, reduce the available pressure drop across the turbine. The turbine efficiency governs the conversion from flow energy to mechanical energy, but may also cause swirling flow in the chimney, which may enhance the effect of loss mechanisms. The work presented here is primarily concerned with the stagnation pressure drops in various parts of the chimney and turbine and how they influence the available turbine pressure drop.

3. Literature review

Haaf et al (1983) have described the experimental performance of a solar chimney power plant. Mullett (1987), Pasumarthi and Sherif (1988), and Gannon and Von Backström (2000) and Kröger and Buys (2002) have published theoretical performance estimates, and Gannon and Von Backström (2003), and Von Backström, Bernhardt and Gannon (2003) have presented data measured on a model turbine and chimney scale models. Few investigators have looked at the influence of secondary effects, but Kröger and Blaine (1999) derived theoretical models for the effects of ambient conditions on the driving potential of solar chimney power plants.

4. Objectives

The main objectives of the study are to bring together and evaluate the magnitudes of the secondary effects listed below, and investigate their influence on the performance of solar chimney power plants:

- Collector-to-chimney-transition loss
- Turbine efficiency
- Wall friction loss
- Chimney internal bracing wheel loss
- Chimney exit loss
- Non-adiabatic atmospheric conditions

The general objective will be to compare these various effects, in order to guide further research, and determine the ultimate performance potential of solar chimneys.

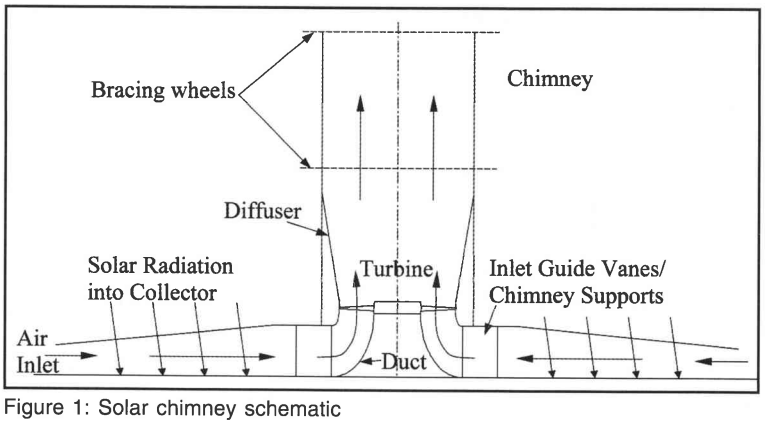

Figure 1: Solar chimney schematic

Department of Mechanical Engineering, University of Stellenbosch, Republic of South Africa
Email: twvb@sun.ac.za

5. Collector-to-chimney transition

The hot air in the solar collector of a solar chimney power plant moves radially inwards towards the chimney. Upon reaching the chimney it turns from the horizontal to the vertical direction in a transition section. The chimney must be supported on a foundation structure consisting of walls or pillars to allow air to enter at its bottom. A previous estimate of the collector-to-chimney transition loss coefficient (with reference dynamic pressure based on turbine cross-sectional area) is 0.25, (Kröger and Buys, 2002).

Gannon and Von Backström (2003) measured the turbine inlet losses in a model chimney rig. Due to laboratory roof height constraints a shortened turbine diffuser expanded to a reduced diameter, 800 mm diameter chimney. The nominal model chimney diameter was 900 mm, giving a scale factor of 1:177.6 relative to a 160 m diameter full-scale chimney. The model collector roof height was 320 mm and the 18 inlet guide vanes (IGVs) had 225 mm chord lengths and they were staggered at 22.5°. The model turbine ran at a tip speed of 45.0 m/s compared to 88.4 m/s envisaged for the prototype.

Gannon (2002) included the losses across the inner part of the solar collector from a radius of 2.25 m, and through the IGVs supporting the chimney in the collector-to-chimney transition loss. He reported a loss coefficient of 0.043 referred to the dynamic pressure based on the turbine inlet velocity. Table 1 presents various flow areas and dynamic pressures in the model. They are useful in when non-dimensionalising with reference to various sections in the system. Figure 2 shows pressure measurements immediately below and above the turbine rotor. The higher pressures are below (upstream of) the rotor, and the pressure difference across the turbine rotor is about 1000 Pa.

The value of the collector-to-chimney transition loss changes to 0.047 when referred to the axial velocity through the turbine, and to $(0.636/0.342)^2 \times 0.047 \approx 0.163$ when referred to the nominal chimney dynamic pressure. Kirstein (2004), using the same configuration and same rig as Gannon, found that the two loss coefficients were 0.040 and 0.138 respectively. It turned out that it was extremely difficult to measure the loss coefficients accurately as they were as low as a few percentage points of the dynamic pressure. Using an estimated model collector inlet loss coefficient of 0.1 and IGV loss coefficient of 0.03 their contributions to the total loss coefficient are estimated to be $(0.636/4.524)^2 \times 0.1 \approx 0.002$ and $[0.636/(0.804 \times \cos 22.5^0)]^2 \times 0.03 \approx 0.022$. The collector-to-chimney transition loss coefficient based on chimney velocity is thus determined as $0.138 - 0.002 - 0.022 \approx 0.114$.

Von Backström (2003) refers to a reference solar chimney with a diameter of 160 m and flow area of 20 106 m^2. For a flow of 250 000 kg/s at density = 0.9695 kg/m^3 the chimney through-flow velocity is 12.82 m/s, the dynamic pressure is 79.7 Pa and the collector-chimney-transition pressure loss is $0.114 \times 79.7 = 9.1 \approx 9$ Pa. This is 0.9 % of the 1000 Pa pressure drop in the reference plant. With the 0.25 coefficient based on turbine cross sectional area (Table 1) it would have been $(0.25/0.114) \times (0.636/0.342)^2 \times 9.1 \approx 69$ Pa, or 6.9 %. Measurements and CFD calculations by Kirstein (2004) confirmed these low values, but indicated even lower values at full scale. Since the full scale chimney is 177 times larger than the model (and density and viscosity are also slightly different) the full scale friction coefficients can be expected to be about 1.8 times lower. The loss coefficients referred to the chimney and turbine dynamic pressures then respectively become $0.114/1.8 = 0.063$ and $(0.342/0.636) \times 0.063 = 0.034$. By using CFD, Kirstein (2004) derived a semi-empirical equation for collector-to-chimney loss coefficient over the whole range of collector-height-to-chimney-diameter ratios, H between 0.2 and 0.4 and inlet guide vane setting angles, β between 0 and 35°.

$$C_{TS} \approx 0.0292 + 0.00114\left(\frac{\sec\beta}{H}\right)^2 + 0.01076\left(\frac{\tan\beta}{H}\right)^2$$

Research aimed at reducing the pressure drop in the collector-to-chimney transition section further is not recommended at this stage, since the loss coefficient is very low and the work of Kirstein (2004) is applicable to a wide range of solar chimney transition section geometries.

Section	Model inlet	IGV exit	Turbine inlet	Nominal Chimney
Flow Area m²	4.524	0.804	0.342	0.636
Dynamic pressure	0.57 Pa	18.1 Pa	100 Pa	28.9 Pa

Table 1: Flow areas and dynamic pressures at four sections in model solar chimney turbine rig

Configuration	IGV +Rotor	IGV +Rotor +short diffuser	IGV +Rotor +long diffuser	Rotor +long diffuser
Efficiency %	91.9	90.2	89.6	90.7

Table 2: Measured total-to-total turbine efficiencies

6. Turbine efficiency

Previous estimates of turbine efficiency were around 80 %, as mentioned by Von Backström and Gannon (2001). The values from the literature were presumably total-to-total values, since in most simple analyses the turbine efficiency is merely seen as the ratio between turbine output power and turbine fluid power. Based on theoretical considerations Von Backström and Gannon (2001) estimated that turbine total-to-total efficiency may be as high as 90 %. This was confirmed recently by Gannon and Von Backström who have reported total-to-total efficiencies of 85 –

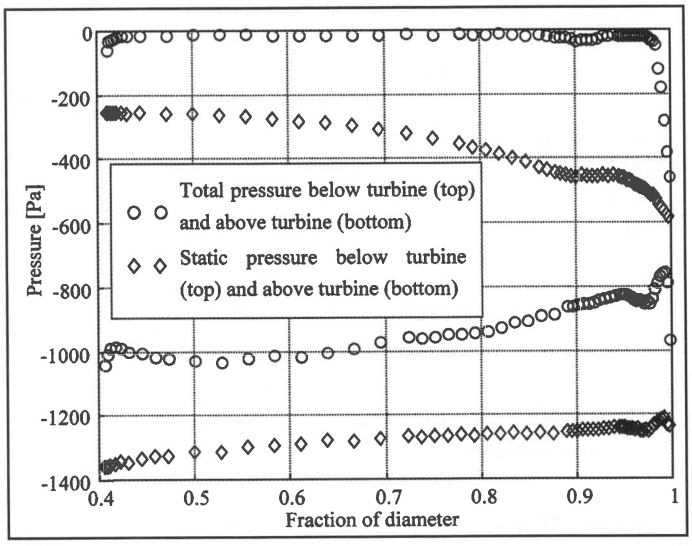

Figure 2: Total and static pressure profiles below and above the turbine (Gannon, 2002)

90 % and total to static efficiencies of 77 – 80 %, as measured in the 0.72 m diameter model turbine.

Table 2 summarises the measured values of efficiency. Except for the value in the last column, these efficiencies include the inlet guide vanes supporting the chimney and the collector-to-chimney transition. As seen in section 5 above, the loss is 0.9 % of the turbine total-to-total pressure drop or, for the full-scale turbine, about 9 Pa, depending on the operating point of the turbine. If the collector-to-chimney transition, (including the IGVs) is not considered as part of the turbine, the turbine efficiency increases by 0.9 %.

7. Chimney internal bracing wheel loss

Von Backström, Bernhardt and Gannon (2003) investigated the flow through a representative tall solar chimney with internal bracing wheels. They presented experimental data measured in a 630 mm diameter laboratory scale chimney model with and without bracing wheels. The seven model bracing wheels each had twelve spokes, each spoke consisting of a pair of rectangular section bars (Figure 3).

A fan at one end of the chimney model either sucked or blew the flow through it (Figure 4). The sucked-through flow entered

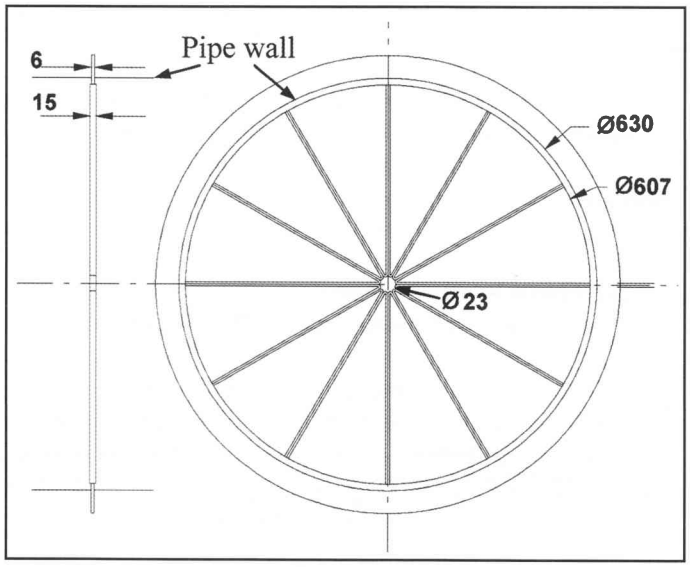

Figure 3: Chimney model bracing wheel

through an elliptic wall section nozzle, ensuring uniform, non-swirling flow. The blown-through flow entered the chimney through a fan and diffuser, resulting in a swirling non-uniform flow, representing the flow leaving the turbine.

Their conclusions were:

- Due to the developing nature of the flow in the chimney, the measured friction pressure drop was 30 % higher than the theoretical values for smooth walls, and swirling, blown flow

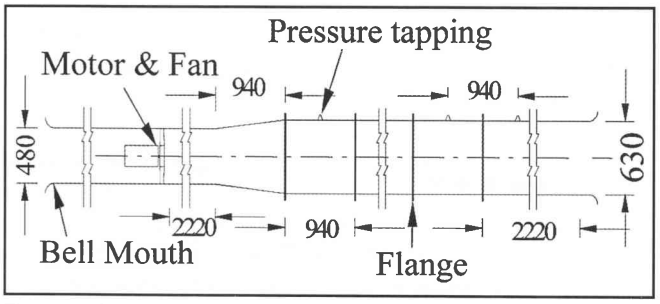

Figure 4: Solar chimney model

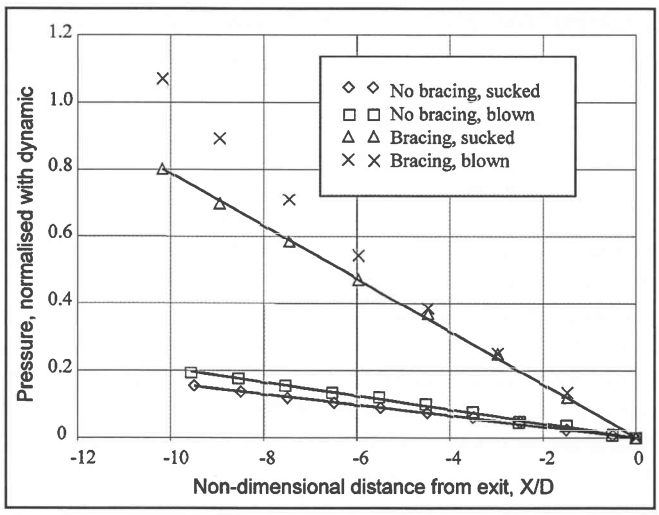

Figure 5: Pressure variation in chimney with and without bracing wheels

increased it by another 25 %.

- The bracing wheels caused order of magnitude larger pressure drops than wall friction. For the blown flow the forced, swirling, disturbed flow increased the pressure drop by up to 36 % (Figure 5), or 25 Pa, representing 2.5 % of the turbine pressure drop.
- With the last wheel at the chimney top, the exit kinetic energy coefficient increased from about 1.12 to 1.26, thereby increasing the exit loss for the reference chimney from 89 to 100 Pa. The increase of 17 Pa represents 1.7% of the turbine pressure drop.

8. Relative contribution to pressure drop of rims and spokes

Von Backström et al. (2003) estimated that for the design under consideration, 70 % of the pressure drop of the bracing wheels was due to the wheel rims protruding 3.65 % of the chimney radius into the chimney, and 30 % due to spoke drag. Using the experimental chimney described in Von Backström et al. (2000), but removing the spokes (but not the rim) of one bracing wheel the chimney pressure drop was measured again. The results in Figure 6 show that the pressure gradient lines up- and downstream of the spokeless wheel are offset by 30 % of the pressure drop between two normal wheels, as expected. The large relative contribution of the wheel rim drag has not been demonstrated before.

This shows that the major effort should be directed towards the reduction of rim drag, rather than spoke drag. In principle the

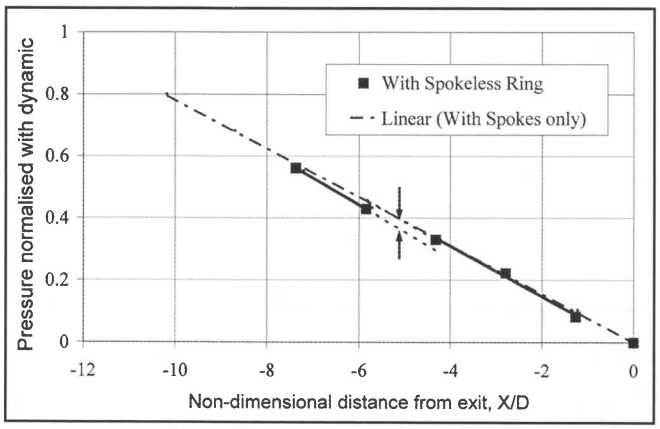

Figure 6: Pressure drop across spokeless bracing wheel

protruding rims should either be removed or replaced with externally protruding rims, or be streamlined. Streamlining would in effect give the rim protrusion the same shape as a venturi wall. The diffuser of the venturi, with an area ratio of 1: (1-0.0365) = 1.0379 would, with a loss coefficient of 0.05, suffer a normalised stagnation pressure loss of $0.1 \times 1.0379^2 \times 7 = 0.38$ over 7 bracing wheels. This is only a 50 % reduction and it clearly shows that inward-protruding bracing wheels rims should be removed (compare to Figure 5) rather than streamlined. This general recommendation is applicable to all chimneys. By dividing the chimney internal losses up into skin friction and bracing wheel spoke losses, the determined loss coefficients can be applied to chimneys with a wide range of distances between the bracing wheels, and to bracing wheels with a wide range of total frontal area as fraction of the chimney area.

9. Effect of spoke streamlining and angle of attack

No applicable literature could be found on the reduction of drag in paired profiles. Spoke drag coefficients were determined by measuring velocity profiles in the wakes of model spoke sections in a wind tunnel with a cross section of 1.4x1.0 m, as described by Von Backström et al. (2002). As shown in Figure 7 there were three different sections each consisting of a pair of bars, namely the original rectangular section, the rounded-nose section and the streamlined section. The streamlining was restricted by the attachment bolts in the experimental set-up, but it is a good example of what can be achieved effectively in practice.

The rectangular section drag coefficient was 0.91. Merely rounding the nose reduced the drag coefficient to 0.56, and

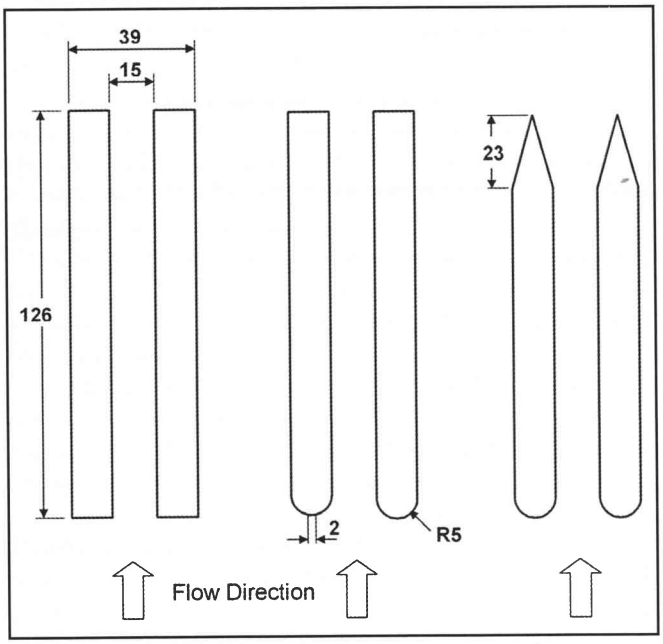

Figure 7: Spoke Sections sized for wind tunnel experiments

Loss mechanism	Wall friction	Wall friction, swirling flow	Bracing wheel	Bracing wheel, swirling flow
Coefficient	0.0110	0.0137	0.0897	0.122
Loss (Pa)	7.0	9.9	69.3	94.3

Table 3: Measured loss coefficients and losses applied to reference chimney

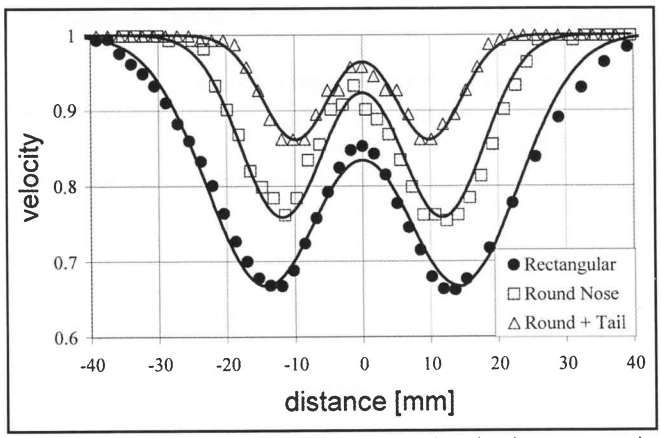

Figure 8: Wake profiles measured behind spoke wheels at zero angle of attack

tapering the tail as well, reduced it further to 0.29, representing about 10 % of the bracing wheel drag. Figure 8 shows the corresponding velocity profiles, with the sum of two offset Gaussian distributions fitted through each of them. Gaussians describe single far field wakes well (White, 1991), but superimposing them to find the drag of two sections close to each other is, as far as could be determined, a novel approach, applicable to many chimney bracing wheel designs and even to the area of mine ventilation.

Figure 9 shows how easily gains achieved by streamlining the spokes can be lost again by swirling flow in the chimney causing the flow to meet the spoke pair at an angle of attack, α. The high drag coefficients of the streamlined spoke for $\alpha = 5$ and 10° of 0.43 and 0.93 were mainly caused by separated flow on the lee side of the lee spoke of the pair. These increased drag coefficients explain in principle the large negative effect of swirling flow in the chimney on the pressure drop through it, as seen in Figure 5.

Taking the chimney dynamic pressure of 79.7 Pa and the loss coefficients from Von Backström et al. (2003), results in Table 3.

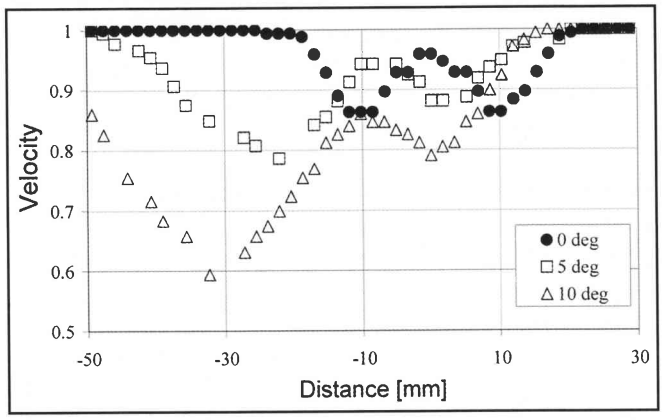

Figure 9: Wake profiles behind streamlined spokes as affected by angle of attack

It shows the pressure drop across ten bracing wheels as 69.3 Pa for non-swirling flow. If the drag coefficient of the spokes is reduced from 0.91 to 0.29 the 30 % of the loss associated with the spokes is reduced to 10 % and the total loss is reduced to (70+10)/(70+30)×69.3 = 0.8 x 69.3 = 55.4 Pa, a reduction of about 14 Pa or 1.4 % of the pressure drop across the turbine. If however, the bracing wheel rims are buried in the chimney walls the reduction is 0.7 x 69.3 = 48.5 Pa, or almost 5 % of the turbine pressure drop.

The spoke pressure drop of 20.8 Pa can be reduced to 7 Pa by streamlining, and designing the turbine for little exit swirl, representing another 1.4 % of turbine pressure drop.

Describing the chimney loss mechanisms in terms of collector-to-chimney loss, skin friction loss, bracing wheel rim loss, bracing wheel spoke loss and exit dynamic pressure loss makes it possible to apply the determined loss coefficients to any chimney geometry.

10. Non-adiabatic atmospheric conditions

The solar chimney thermodynamic cycle is similar to that of a gas turbine. The solar collector represents the combustor and the solar chimney turbine the power turbine. In a gas turbine the gas generator turbine extracts energy to drive the turbine, but in the solar chimney turbine the chimney converts enthalpy to potential energy and releases the air at the top of the chimney. The surrounding ambient air descending in an imaginary chimney represents the compression part of the thermodynamic cycle. The usual assumption for dry desert conditions is that of adiabatic compression, and since the compression may also be regarded as frictionless, it is effectively isentropic. If, however, it is assumed that standard conditions describe the ambient atmosphere, the compression process is polytropic, and it represents intercooled compression. Intercooled compression generally benefits compression processes since it reduces the volume flow and power required in subsequent stages of the compression process. It does not generally enhance a gas turbine cycle, since it removes heat from the cycle, with the consequence that more heat must be added in the combustor or in the solar collector.

Kröger and Blaine (1999) derived theoretical models for the effects of ambient conditions on the driving potential of solar chimney power plants. They concluded that, compared to adiabatic atmospheric conditions, standard atmospheric conditions are detrimental to the performance of the chimney. The basic reason is their assumption of equal ground level conditions in the two atmospheric models. Since the temperature in the standard model decreases by 6.5°C per 1000 m compared to 9.76°C per 1000m in the adiabatic model, the average ambient temperature along the chimney height is higher, the density lower and the driving potential is smaller.

Consider for example the following conditions taken from US Standard Atmosphere Table (White, 1991) at 1000 m and 2500 m above sea level:

Ground level (1000 m): temperature t_2 =281.66 K, pressure, p_2 = 89.889 kPa, density, ρ = 1.1120 kg/m^3;

Chimney top level (2500 m): temperature t_3 =271.91 K, pressure, p_3 = 74.684 kPa, density, ρ_3 = 0.9570 kg/m^3.

For an isentropic process, with the same ground level (collector inlet) conditions the corresponding chimney top level values are: temperature t_3 =267.02 K, pressure, p_3 = 74.571 kPa, density, ρ_3 = 0.9731 kg/m3. In the case of the standard atmosphere the ambient pressure at the chimney top is 113 Pa higher, reducing the available pressure drop of about 1000 Pa across the turbine by 11%. This conclusion agrees with Kröger and Blaine (1999).

Component	Pressure drop (Pa)	% of Turbine Pressure drop
Collector-chimney transition	5	0.5
Turbine loss	100	10
Wall friction	9.9	1.0
Bracing wheel rims	48.4	4.8
Bracing wheel spokes	20.8	2.1
Exit	100	10.0
Non-adiabatic atmosphere	113	11.3

Table 4: Component losses and atmospheric effect expressed as % of turbine pressure drop

11. Summary and conclusions

The paper evaluates the absolute and relative contributions of certain secondary effects on the performance of solar chimney power plants. Table 4 expresses the contributions of the various components of the chimney in terms of turbine efficiency percentage points. The table shows that the relative influence of several secondary effects on the pressure potential across the turbine. Bracing wheel rim drag, which also affects the exit loss, is the most important, but most of the effects are much smaller than the influence of the ambient atmospheric lapse rate. The sum of all the secondary losses, except the exit loss is 14 % of the turbine pressure drop.

With the removal of the bracing wheel rim, as recommended, the only remaining effect larger than 1 % of the turbine pressure drop is the drag of the bracing wheel spokes, and the exit dynamic pressure.

The main conclusions are the following:

1. The collector-to-chimney transition loss coefficient, referred to chimney flow area is 0.063 (excluding inlet guide vane loss). This is 0.5 % of the turbine pressure drop at design.
2. Turbine total-to-total efficiencies of around 90 % are possible.
3. The pressure drop due to chimney skin friction is 1 % of the turbine design value.
4. Bracing wheel rims could account for 70 % of the bracing wheel loss and the rectangular section spokes for 30 %. Rim loss can be eliminated by removing the inward protruding rims.
5. Rounding off the spoke leading edges could reduce the spoke drag coefficient from 0.91 to 0.56 and tapering the rear 18 % of the tail too, can further reduce it to 0.29.
6. The drag coefficient of the streamlined spokes increased to 0.43 at an angle of attack of 5° and to 0.93 at 10°, showing the large negative effect of swirling flow on bracing wheel drag.
7. A standard type atmosphere with a lapse rate of 6.5 K per 1000 m reduces the available pressure drop across the turbine by about 11 % for the reference 1500 m tall chimney, compared to an adiabatic atmospheric model.

Comparing the system pressure losses with the possible effects of atmospheric conditions shows that very limited scope remains for improving the performance of solar chimney power plants by reducing secondary losses in the system. The ultimate system pressure drop, excluding losses in the collector is about 1.5 times the chimney exit dynamic pressure.

The findings presented in this paper are intended as a concise source of information to be used in design and optimisation studies of chimneys for solar chimney power plants.

References

❑ Gannon, A.J. and Von Backström, T.W. (2000). Solar chimney analysis with system loss and solar collector performance. *ASME Journal of Solar Energy Engineering,* 122,

133-137.

- Gannon, A.J. (2002). Solar chimney turbine performance. *PhD dissertation, University of Stellenbosch, March 2002.*
- Gannon, A.J. and Von Backström, T.W. (2003). Solar chimney turbine performance. *ASME Journal of Solar Energy Engineering,* 125, No. 1, 101-106.
- Haaf W, Friedrich K, Mayr G and Schlaich J. (1983). Solar chimneys Part 1: Principle and construction of the pilot plant in Manzanares. *International Journal of Solar Energy,* 2 , 3-20.
- Kirstein, C.F., "Flow Through a Solar Chimney Transition Duct", 2004, Master's Thesis, Department Mechanical Engineering, University of Stellenbosch, Stellenbosch, South Africa.
- Kröger, D.G. and Blaine, D. (1999). Analysis of the driving potential of a solar chimney power plant, *S.A.I.Mech.E. R&D Journal,* 15, 85–94.
- Kröger, D.G. and Buys, J.D. (2002). Solar chimney power plant characteristics, *S.A.I.Mech.E. R&D Journal,* 15, 31–36.
- Mullett LB. (1987). The solar chimney - overall efficiency, design and performance. *International Journal of Ambient Energy,* 8, No 1, 35-40.
- Pasumarthi N and Sherif, SA. (1988) Experimental and theoretical performance of a demonstration solar chimney model – Part I: Mathematical model development. *International Journal of Energy Research,* Vol 22, 277-288.
- Schlaich J. (1995). *The solar chimney, electricity from the sun.* Axel Menges, Stuttgart, Germany, pp.6-52.
- Von Backström, TW and Gannon, AJ. (2000). Compressible flow through solar power plant chimneys. *ASME Journal of Solar Energy Engineering,* 122, 138-145.
- Von Backström, T.W. (2000). The solar chimney air standard cycle. *SAIMechE R&D Journal,* 16, No 1, 16-24.
- Von Backström, T.W., Bernhardt, A. and Gannon, A.J. (2003). Pressure drop in solar power plant chimneys. *ASME Journal of Solar Energy Engineering,* 125, No. 2, 165-169.
- Von Backström T.W. and Gannon, A.J., Solar chimney - turbine characteristics, *ISES Solar Energy Journal, Special Proceedings Issue,* 76, Issues 1 3, pp. 235 241, January March 2004.
- Von Backström T.W. (2003). Calculation of pressure and density in solar power plant chimneys. *ASME Journal of Solar Energy Engineering,* 125, No. 1, 127-129. (Technical Brief).
- White, F.M., (1991). *Viscous fluid flow,* 2nd edn. p. 479. McGraw-Hill.